

TEMPERATURE CALIBRATION OF A MASS SPECTROGRAPHIC EVOLVED GAS ANALYSIS SYSTEM *

P.K. GALLAGHER

AT & T Bell Laboratories, Murray Hill, NJ 07974 (U.S.A.)

(Received 16 July 1984)

ABSTRACT

Because of the vacuum used in mass spectrographic evolved gas analysis, the usual effects of temperature lag between actual and apparent sample temperatures are exaggerated. Factors contributing to this temperature difference are discussed. The melting point of various metals in the range 110–1100 °C are used to obtain insights and estimates regarding these temperature discrepancies at different heating rates, utilizing a variety of sample holders. In general, if the sample is in good contact with the heated supporting surface, the agreement between the observed and reported equilibrium melting temperatures is good at heating rates of $\leq \sim 20$ °C min. At higher heating rates the differences become larger (≥ 10 °C) and the effect increases with increasing temperature of melting. For sample holders which are not in good contact with the sample, hot spots can develop at high temperatures due to unequal thermal radiation. Under these circumstances the apparent melting point can be considerably lower than the actual equilibrium temperature and less dependent upon heating rate.

INTRODUCTION

Evolved gas analysis (EGA), particularly that utilizing mass spectroscopy, has grown dramatically in popularity in recent years. It has been utilized in such diverse applications as: (1) to characterize the product from the decomposition of bulk materials, e.g., arsenates [1]; (2) to determine the species evolved during the pyrolysis of organic or organometallic compounds [2]; (3) to follow the rate of III–V semiconductor decomposition [3,4]; and (4) to evaluate the impurity species in thin films [5,6]. The high sensitivity and specificity of the technique, as compared to the more conventional determinations of changes in weight or heat, have made it an invaluable technique amongst the collection of conventional thermoanalytical methods.

One of the major concerns in the application of mass spectrographic EGA is the accurate determination of the sample temperature. The nature of the mass spectrographic method typically requires the application of reasonably

* Presented at the 13th Annual NATAS Meeting, Philadelphia, PA, 24–26 September, 1984.

good vacuums (10^{-4} – 10^{-8} Torr). Under these conditions thermal conduction is generally impeded and consequently the temperature lags between sample, measuring thermocouple, and furnace are exaggerated. Because high temperatures and reactive samples are frequently used, it is not generally practical to design the apparatus such that the thermocouple and sample are in good physical contact.

The system used in the applications mentioned earlier involves the placement of a shielded thermocouple into a well near the sample in the sample holder [7]. This paper attempts to determine the difference between the actual sample temperature and the measured temperatures as a function of type of sample holder and heating rate over a wide range of temperature (100–1200 °C). One technique which has proved successful for other methods of EGA has been the abrupt evolution of occluded volatile impurities during the first-order solid₁ → solid₂ phase transition. An example is ethanol, or 1,4-dioxane from such materials as KNO₃, KClO₄ or K₂SO₄ [8]. This method is not expected to be generally successful for mass spectrographic EGA, however, because of the difficulty in retaining the impurity to the transition temperature, in the vacuum required by the method. This unsuitability is verified herein.

A different scheme utilizing the melting point is tested. The premise is that although there is usually not a discontinuity in the vapor pressure of a material upon passing through its melting point, there is generally a reduction of available surface due to surface tension drawing towards a spherical shape. Either a possible discontinuity or a significant reduction in available surface should lead to an irregularity in the mass spectrographic signal associated with that particular species. A suitable variety of metals was used to cover the wide temperature range from 100 to 1200 °C.

EXPERIMENTAL PROCEDURES AND RESULTS

The basic mass spectrographic EGA apparatus has been previously described [7]. Certain relevant updates, however, have been made. The current temperature programmer/controller consists of a Eurotherm Model 984/932 controller and power supply, while the programmer signal is provided by an Iveron Model 2100A. The sensor is an Inconel-sheathed chromel/alumel thermocouple and the upper temperature limit of the system is 1200 °C. A UTI programmable peak selector is used to gather digital data and control the mass spectrometer. As many as nine peaks can be simultaneously monitored but two of the nine channels are invariably used to record the temperatures and total pressure. The total pressure signal is from the analog output of a Perkin-Elmer DGC III gauge controller. Both the temperature and pressure outputs are amplified ($\times 10$) (Spectrum Model 1021) prior to input into the data acquisition chain. Upon completion of the experiment

the data are transferred via an RS232C link to a Fluke Model 2452 based microcomputer system for data manipulation, listing, plotting, and archival.

The basic sample holder consists of an alumina crucible (~ 1 cm ID, ~ 1.25 cm in height) into which a variety of inserts are placed. The three major types of inserts are shown in Fig. 1. Type A is used for powders or small fragments and employs either alumina or platinum inner crucibles. Types B and C are used for supported thin films. Generally, an 8×5 mm rectangular substrate/film sample is used with type B, while an approximately 4 mm disk is preferred for type C.

Fine crystalline K_2SO_4 doped with 1,4-dioxane was prepared by forcing K_2SO_4 from a saturated aqueous solution with the rapid addition of three times the aqueous volume of 1,4-dioxane. The resulting material was filtered and dried overnight at 100°C . About 20 mg of this material was loaded into a type A holder with an alumina inner crucible and heated at $10^\circ\text{C min}^{-1}$ to 750°C . The 1,4-dioxane gave a broad peak below 300°C and had completely disappeared by the time the solid-state transition of K_2SO_4 at 583°C was reached. Since 1,4-dioxane was the least volatile species proposed for this general method [8], it was concluded that the technique was not suitable for application in vacuum.

The approach was then shifted to look for discontinuities in vapor pressures during melting. Occasionally, there were spectacular results enabling the clear association of the event with the melting point of the metal. Such a result is shown in Fig. 2 for a piece of high-purity Al wire heated at $10^\circ\text{C min}^{-1}$ in the type A holder with an alumina inner crucible. More typical results, however, are shown in Fig. 3 for several heating rates. Similar results for high-purity Sn and In in the type A holder are presented in Figs. 4

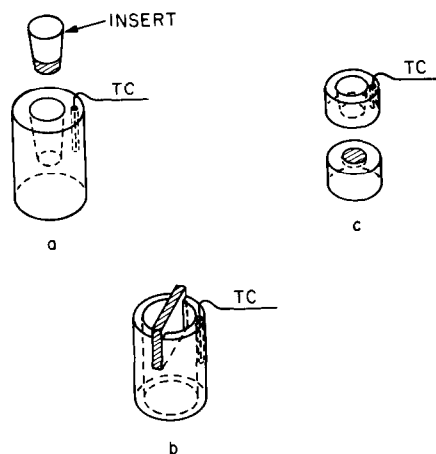


Fig. 1. Type of sample holders: (a) Al_2O_3 cylinder with Al_2O_3 or Pt inserts, sample: powder; (b) slotted sapphire tube, sample: $\sim 5 \times 8$ mm rectangle; (c) graphite two-piece (bottom, cylinder; top, tube), sample: ~ 4 mm diameter disk. TC = chromel/alumel thermocouple, hatched area = sample.

and 5, respectively. Figure 6 indicates how the sensitivity or amplification setting on the mass spectrometer can influence any subjective evaluation of the onset of evolution.

Results on the graphite block (type C) holder are shown at several heating rates in Figs. 7 and 8 for high-purity Sn and Cu, respectively. The melting of Cu also leads to an enhanced evolution of O_2 as seen in Fig. 9.

Finally, some results are shown in Figs. 10 and 11 using the slotted sapphire holder (type B) for Sn and Cu foils.

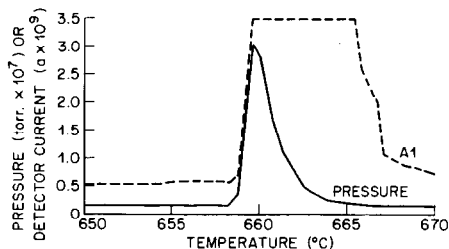


Fig. 2. An atypical example of Al evolution at its melting, type A holder (12.15 mg Al at $10^\circ\text{C min}^{-1}$): (-----) AMU = 32, amplification of $\times 10^9$; (—) total pressure (Torr $\times 10^{-7}$).

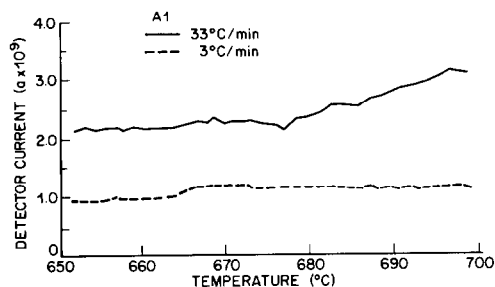


Fig. 3. Typical example of Al evolution at its melting, type A holder: (—) 7.91 mg Al, $33^\circ\text{C min}^{-1}$, AMU = 27, amplification of $\times 10^9$; (-----) 9.33 mg Al, 3°C min^{-1} , AMU = 27, amplification of $\times 10^9$.

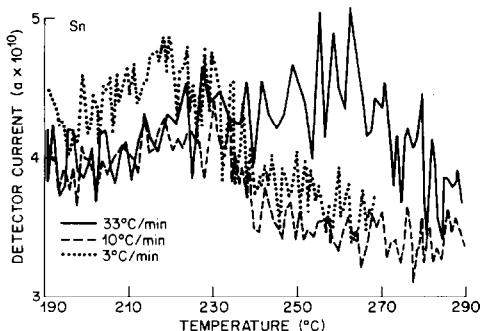


Fig. 4. Sn evolution through its melting, type A holder (AMU = 115, amplification of $\times 10^{10}$): (—) 82.13 mg, $33^\circ\text{C min}^{-1}$; (-----) 92.85 mg, $10^\circ\text{C min}^{-1}$; (.....) 41.63 mg, 3°C min^{-1} .

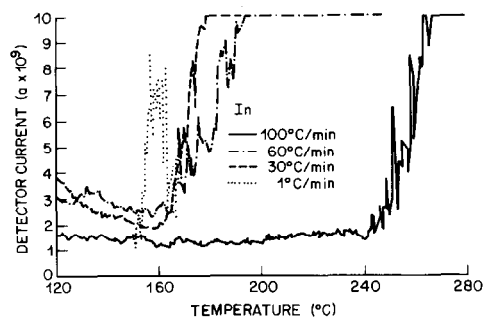


Fig. 5. In evolution through its melting, type A holder (AMU = 115, amplification of 10^9): (—) 45.12 mg, $100^\circ\text{C min}^{-1}$; (-·-·-) 61.40 mg, $60^\circ\text{C min}^{-1}$; (- - - -) 42.39 mg, $30^\circ\text{C min}^{-1}$; (· · · · ·) 47.33 mg, 1°C min^{-1} .

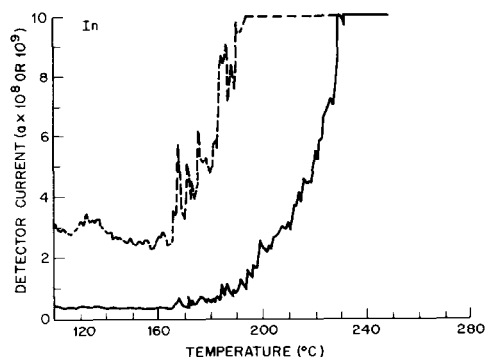


Fig. 6. In evolution through its melting, type A holder (AMU = 115, 60°min^{-1}). (—) $\times 10^8$; (- - - -) $\times 10^9$.

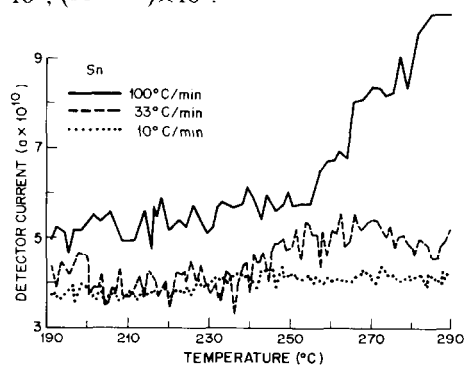


Fig. 7. Sn evolution through its melting, type C holder (AMU = 120, amplification of 10^{10}): (—) 54.00 mg, $100^\circ\text{C min}^{-1}$; (- - - -) 39.73 mg, $33^\circ\text{C min}^{-1}$; (· · · · ·) 32.09 mg, $10^\circ\text{C min}^{-1}$.

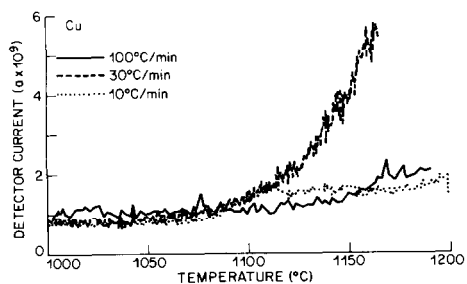


Fig. 8. Cu evolution through its melting type C holder (AMU = 63, amplification of 10^9): (—) 38.32 mg, $100^\circ\text{C min}^{-1}$; (- - - -) 37.37 mg, $30^\circ\text{C min}^{-1}$; (· · · · ·) 38.95 mg, $10^\circ\text{C min}^{-1}$.

DISCUSSION

Sources of error are listed in Table 1. The first two of these are dependent upon sample size, nature of the reaction, quality of vacuum, region of temperature, and the particular thermal characteristics of the furnace, holder, thermocouple and sample combination. In addition, because of the close proximity of the sample holder to the ionizing filaments of the mass spectrometer, there is the complication of radiant heat transfer from the

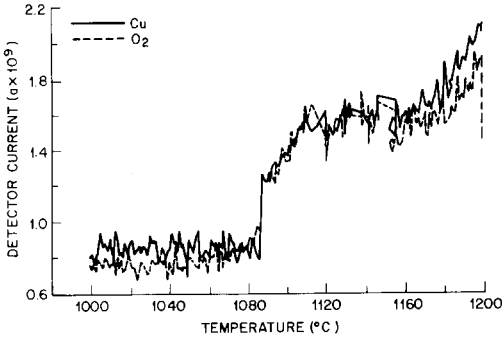


Fig. 9. Cu and O₂ evolution through the melting of Cu, type C holder (10°C min⁻¹, amplification of 10⁹).

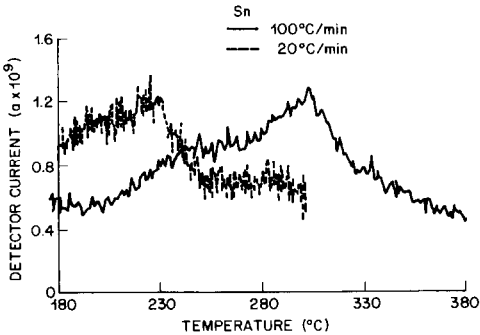


Fig. 10. Sn evolution through its melting, type B holder (AMU = 120, amplification of 10⁹).

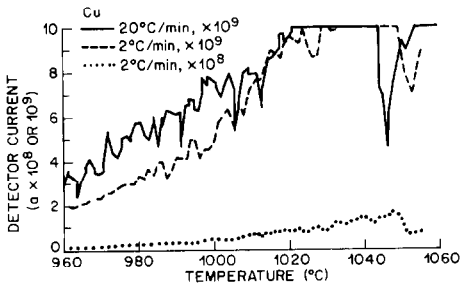


Fig. 11. Cu evolution through its melting, type B holder (AMU = 63).

TABLE 1

Sources of temperature error in mass spectrographic EGA

-
- (1) Separation of the sample and temperature sensor
 - (2) Enthalpy of various transitions and reactions
 - (3) Instrumental inaccuracies
 - (a) Thermocouple calibration
 - (b) Amplification, linearization, etc., within the temperature controller
 - (c) A to D conversion by the data acquisition system
-

filaments. The instrumental inaccuracies (factor 3) are not dependent on the experimental conditions described above and hopefully represent a much smaller and relatively constant error. Determination of the actual rise in intensity above background is a very subjective measurement and dependent upon the degree of amplification as will be shown later. Use of more readily evaluated criteria such as the extrapolated onset (intersection of the slope at the point of inflection in the rise with the extrapolated baseline), as commonly used in DTA measurements, is possible and clearly reveals a trend with heating rate. The sensitivity of the technique is markedly increased at faster heating rates. Although the quantity of evolved gas may be the same, the gas is evolved in a shorter period of time during rapid heating and the constant pumping speed allows the partial pressure to reach a higher value. While this increased sensitivity is valuable, it is offset by the temperature lag between the sample temperature and measuring thermocouple. This then indicates one of the major compromises that must be achieved in this type of measurement, similar to DTA. In those cases where precise temperature is most important, slower heating rates should be used but for cases of qualitative detection, higher heating rates are valuable to reduce both the quantity of sample needed and the time necessary to conduct the experiment.

It is unfortunate that the relatively unambiguous evolution of solvent at the solid₁ → solid₂ phase transition of K₂SO₄ did not work. This would have provided a sharp evolution at a well-defined temperature. It was, however, optimistic to expect the trapped or occluded solvent to remain to the transition temperature in the vacuum present in the mass spectrometer system, unlike that attainable during EGA at atmospheric pressure [8].

Solid-state transitions which evolve naturally absorbed gases are rare. However, it was found possible to detect changes in partial pressures upon melting a number of metals. In rare inexplicable occurrences these effects are particularly dramatic, such as that observed in Fig. 2 for a piece of Al wire. The sharp increase in the Al partial pressure was also reflected in the total pressure. A possible explanation may be associated with a catastrophic breakdown of the inherent protective layer of oxide. The much less pronounced effects shown in Fig. 3, however, are far more typical. The dif-

ference in sensitivity and thermal lag between the two heating rates is evident. The extrapolated onset of the offset seems to be at about 662 and 677 °C for 3 and 30 °C min⁻¹, respectively. This is in good agreement with the generally accepted equilibrium melting point of 660 °C. Intuitively, a decrease in the Al partial pressure would be expected as the sample's surface area decreases upon melting due to surface tension. However, the breakdown of the protective oxide film is probably the reason for the observed increase in Al partial pressure. This effect is also noted for some other metals in this work.

The anticipated behavior is indicated by melting Sn in Fig. 4. The extrapolated onset of the decrease in partial pressure of Sn occurs very near the equilibrium melting point of the metal at 232 °C for the two slowest heating rates of 3 and 10 °C min⁻¹ but some 30–35 °C higher at the fastest heating rate of 33 °C min⁻¹. The apparent vapor pressure of In, however, again behaves in the unexpected fashion of increasing quite dramatically upon melting, as seen in Fig. 5. The apparent dependence of the onset of evolution upon the degree of amplification is clearly evident in Fig. 6 where the data were independently collected during the same experiment but at different amplification settings of the mass spectrometer. For this reason it is necessary to make comparisons at the same degree of amplification as in preceding figures.

The data for this particular sample holder configuration are summarized in Table 2. Generally, there is little deviation from the accepted equilibrium melting points when heating at rates of ≤ 10 °C min⁻¹. At more rapid rates the departure is more evident and tends to be higher at higher temperatures with increasing heating rates.

The type C holder assures a reducing atmosphere by placing the sample in contact with graphite. Thermally it is similar to type A except that it is in two pieces and made of graphite rather than alumina. Qualitatively the

TABLE 2

Summary of apparent melting temperatures (°C) in type A sample holders with Al₂O₃ insert crucibles (parenthetic values are differences from the equilibrium value)

Heating rate (°C min ⁻¹)	Sample		
	Al	Sn	In
100			250 (+ 84)
60			170 (+ 14)
33		265 (+ 33)	
30	677 (+ 17)		167 (+ 11)
10		232 (0)	
3	662 (+ 2)		
1			153 (- 3)
Equilibrium	66	232	156

results in Figs. 7 and 8 are similar to those shown earlier. The results are summarized in Table 3. Thermal conduction appears to be better in that the thermocouple reads a little high at $10^{\circ}\text{C min}^{-1}$ and the differences at the faster rates are not as great as for the type A holder. Again the differences are more marked at the higher temperature. The behavior of Cu is interesting in that oxygen is also released on melting (see Fig. 9). The perfect correspondence in the rise of partial pressure for the two components is virtually indistinguishable and lends credence to this point representing a specific transition as opposed to a simple vapor pressure curve for Cu.

The behavior observed for both these materials, Sn and Cu, in the type B holder is remarkably different. In the type B holder the sample is a 5×8 mm sheet or foil which is not in direct contact with the sample holder except at its edges. When it melts there is indeed a large change in surface area and the sample also falls to the bottom of the furnace. This leads to the expected, abrupt drop in partial pressure of the metal, as can be seen in Figs. 10 and 11. Unfortunately, the choice of amplification was not ideal in the case of Cu (Fig. 11) and hence there is some saturation prior to the dropoff. This gives rise to some uncertainty in establishing the exact temperature of the decrease in partial pressure hence the temperature for both rates are upper limits. The temperature is not uniform over the large sample and the results in Figs. 10 and 11 and Table 4 are indicative of what must be the hot spots which presumably arise from uneven heating. The lower-melting Sn exhibits the marked dependence on heating rate seen previously, however, in the Cu case at high temperatures there seems to be little or perhaps even an inverse dependence upon heating rate. In addition, the observed melting temperatures are apparently much below the equilibrium value. The difference between Sn and Cu is probably associated with the greater dependence upon radiant heat transfer at the higher temperature and particularly for this sample holder where most of the sample is not in direct contact with the sample support or holder.

TABLE 3

Summary of apparent melting temperatures ($^{\circ}\text{C}$) in the type C sample holder (parenthetic values are differences from the equilibrium value)

Heating rate ($^{\circ}\text{C min}^{-1}$)	Sample	
	Cu	Sn
100	1131 (+ 48)	250 (+ 18)
33		234 (+ 2)
30	1115 (+ 32)	
10	1082 (- 1)	320 (- 2)
Equilibrium	1083	232

TABLE 4

Summary of apparent melting temperatures ($^{\circ}\text{C}$) in the type B sample holder (parenthetic values are differences from the equilibrium value)

Heating rate ($^{\circ}\text{C min}^{-1}$)	Sample	
	Cu	Sn
100		302 (+ 70)
20	1044 (- 39)	231 (- 1)
2	1047 (- 36)	
Equilibrium	1083	232

CONCLUSIONS

(1) The evolution of trapped or occluded solvent at $\text{solid}_1 \rightarrow \text{solid}_2$ phase transitions is generally not practical for calibrating a mass spectrographic EGA system at elevated temperatures due to the difficulty in retaining the volatile solvent in vacuum until the temperature of the transition.

(2) The melting point of metals can be detected in the mass spectrometer by virtue of changes in vapor pressure resulting from a breakdown in the protective oxide film, a genuine discontinuity in the vapor pressure, or the change in available surface area on collapse of the sample.

(3) When the metal is in good contact with the supporting heated surface, there is good agreement between the observed irregularity in the mass spectrographic signal and the equilibrium melting temperature at heating rates of $\leq \sim 20^{\circ}\text{C min}^{-1}$. At higher heating rates the measurement lag becomes larger and increases with increasing temperature of the effect.

(4) When the metal is not in good contact with the heated support and the thermal transport is very predominantly by radiation, then the effects at higher temperatures may be reversed due to the development of apparent hot spots.

REFERENCES

- 1 P.K. Gallagher, *Thermochim. Acta*, 14 (1976) 131.
- 2 B.G. Bagley, P.K. Gallagher, W.E. Quinn and L.J. Amos, *Mater. Lett.*, in press.
- 3 E. Kinsbron, P.K. Gallagher and A.T. English, *Solid-State Electron.*, 22 (1979) 517.
- 4 L.G. Van Uitert, P.K. Gallagher, S. Singh and G.J. Zyzdik, *J. Vac. Sci. Technol.*, B1 (1983) 825.
- 5 P.K. Gallagher, *Thermochim. Acta*, 41 (1980) 323.
- 6 P.K. Gallagher, *J. Therm. Anal.*, 25 (1982) 7.
- 7 P.K. Gallagher, *Thermochim. Acta*, 26 (1978) 175.
- 8 P.D. Garn and R.L. Tucker, *J. Therm. Anal.*, 5 (1973) 483.